

Material Selection and Fiber Orientation Effects in Composite Overwrapped Steel Pipelines: A Numerical Study for Burst Pressure Enhancement

Samudra Jit Saha¹, Marufa Akter¹, Nowreen Jahan¹, Sayma Islam¹, Abid Chowdhury¹ and Md. Abdus Shabur^{2,*}

¹Department of Robotics and Mechatronics Engineering, University of Dhaka, Dhaka-1000, Bangladesh

²Institute of Leather Engineering and Technology, University of Dhaka, Dhaka-1209, Bangladesh

Abstract: This study establishes a validated finite element framework for optimizing the burst capacity of petroleum-grade steel pipelines reinforced with composite overwraps. Addressing the limitations of classical netting analysis, the research develops a coupled ANSYS Mechanical and ACP workflow to systematically evaluate the influence of fiber orientation on structural integrity. The methodology first validates the static structural approach against Barlow's equation using a thin-walled baseline (100 mm diameter, 3 mm wall), yielding a numerical failure pressure of 15.75 MPa against an analytical prediction of 13.8 MPa. Upon validation, the framework is scaled to a production-grade geometry (168.3 mm diameter, 7.1 mm wall) to execute a parametric sweep of winding angles (25 to 90 degrees) across four material systems: Epoxy E-Glass Wet, S-Glass UD, Carbon UD (230 GPa), and Woven Carbon. The results reveal a critical divergence in failure mechanics governed by fiber topology. Unidirectional systems (Carbon, S-Glass, E-Glass) consistently exhibit a "helical advantage," achieving maximum burst pressure at 25 degrees—with Carbon UD peaking at 51.24 MPa—due to superior shear stiffening and axial confinement. Conversely, Woven Carbon displays a unique recovery trend, maximizing performance at 90 degrees (49.15 MPa) where its bidirectional architecture effectively balances hoop stresses. These findings provide a reproducible "angle-performance map" for field engineers, demonstrating that while low-angle helical wraps are optimal for high-modulus tapes, hoop-dominant configurations are required for woven fabrics, thereby refining design guidelines for in-situ pipeline rehabilitation.

Keywords: Pipeline Repair, Composite Overwrap, Finite Element Analysis, Fiber Orientation, Burst Pressure, Material Selection.

1. INTRODUCTION

The structural integrity of petroleum transportation infrastructure remains one of the most critical concerns for the global energy sector. Steel pipelines serve as the backbone for distributing crude oil and refined products, but they are forced to operate under punishing conditions. These pipes face a constant combination of high internal hydrostatic pressures, corrosive chemical environments, and external mechanical loads [1]. Over time, this exposure leads to inevitable material degradation specifically wall thinning, corrosion pitting, and fatigue cracking which directly compromises the network's Maximum Allowable Operating Pressure (MAOP) [2].

Historically, fixing these issues has been costly and dangerous. Traditional remediation methods, such as cutting out damaged sections or welding on steel sleeves, usually require a complete pipeline shutdown. Even worse, they introduce "hot-work" hazards, which are economically damaging and logistically risky in active oil fields [3]. This reality has driven the industry

toward composite repair systems, specifically Carbon Fiber (CFRP) and Glass Fiber (GFRP) overwraps. These systems offer a superior alternative because they allow for in-situ reinforcement; operators can often restore or even exceed the pipe's original pressure capacity without ever interrupting service [1, 4].

The effectiveness of a composite overwrap relies entirely on the orthotropic nature of the reinforcement. Unlike steel, which has isotropic strength (equal in all directions), a composite layer is only strong where the fibers are pointing. Classical Lamination Theory (CLT) and standard "netting analysis" for cylindrical vessels usually point to a specific "magic angle" of approximately ± 54.7 degrees relative to the longitudinal axis. In theory, this angle perfectly balances the hoop stress and longitudinal stress, which exist in a 2:1 ratio in closed-ended vessels [5, 6]. However, the real world rarely aligns perfectly with theory. Practical applications often deviate from this optimum due to complex factors like layer-to-layer interaction, differences in stiffness ratios (modulus of elasticity), and the specific boundary conditions of the pipeline itself [7]. While there is plenty of existing research using Finite Element Analysis (FEA) to model small patch repairs for localized defects [2, 8], there is a significant lack of comprehensive comparisons

*Address correspondence to this author at the Institute of Leather Engineering and Technology, University of Dhaka, Dhaka-1209, Bangladesh
E-mail: abdusshaur@du.ac.bd

that focus on the global strengthening of pipes using modern, off-the-shelf prepreg systems.

We selected four specific materials—Epoxy E-Glass Wet, Epoxy S-Glass UD, Epoxy Carbon UD (230 GPa), and Epoxy Carbon Woven—to represent the full spectrum of solutions used in the field. E-Glass (Wet) serves as the economic baseline; S-Glass acts as the intermediate step with higher stiffness; and Carbon UD represents the premium, high-stiffness choice for maximum confinement. We also included Woven Carbon to test how weave topology compares to unidirectional laminates. Finally, we designed the simulation with an angular sweep ranging from 25° to 90°. This specific range allows us to capture the full transition of mechanical behavior: from low-angle helical reinforcement (which handles shear and axial loads well) up to pure hoop reinforcement (which aligns with circumferential stresses). This approach allows the study to decouple the material behavior from the classical $\pm 55^\circ$ predictions, systematically identifying the actual optimum wrapping configuration for each composite type based on its interaction with the 0° inner ply.

2. LITERATURE REVIEW

2.1. Composite Repair Systems for Steel Pipelines

Composite overwrap repair has been widely investigated as a non-intrusive alternative to conventional welded interventions for restoring or enhancing the pressure capacity of steel pipelines. Early state-of-the-art assessments emphasized that composite systems can be applied in situ and avoid operational disruption and hot-work hazards, which has driven their adoption in transmission pipeline maintenance [3]. Building on this industry motivation, later research shifted toward quantifying structural benefits and establishing reliable analysis frameworks for repaired pipes. Chen *et al.* demonstrated, through nonlinear finite element modeling of composite-repaired steel pipes, that composite reinforcement can significantly reduce stress concentration around damaged regions and can closely reproduce experimentally observed trends when the modeling is properly calibrated [1]. Esmaeel and Taheri further highlighted that beyond laminate stiffness, the global effectiveness of a composite sleeve strongly depends on how load is transferred through the steel–composite interface, showing that stress redistribution patterns are sensitive to repair configuration and bonding assumptions [4].

2.2. Analytical Guidance for Winding Angle and Its Limitations

The selection of filament-winding or wrapping angle has historically been guided by classical lamination/netting concepts developed for composite pressure vessels. Multi-layer filament-wound pipe studies have shown that laminate orientation governs the balance between hoop and axial stiffness, and that winding angle strongly affects deformation and failure response under internal pressure [5]. Foundational experimental work on $\pm 55^\circ$ filament-wound glass-fiber tubes under biaxial loading contributed to the common “rule-of-thumb” that angles near $\pm 55^\circ$ provide an efficient stress balance in closed-ended cylindrical vessels [6]. However, subsequent research has consistently shown that such analytical guidelines can deviate from optimality once real repair conditions are introduced—particularly when the composite is applied as an external reinforcement over a steel substrate, when the stacking sequence is constrained, or when boundary conditions are not idealized. Sulaiman *et al.* emphasized through numerical studies that internal pressure response is sensitive to modelling assumptions and laminate configuration, motivating the use of finite element analysis for application-specific optimization rather than universal angle prescriptions [7].

2.3. Finite Element Approaches for Wrapped Pipes and Repair Configurations

Finite element analysis has become the dominant tool for studying composite wrapping of steel pipes because it can capture three-dimensional stress states, constraint effects, and steel–composite load sharing. Turai *et al.* investigated wrapping structures using FEA and reported that orientation and modelling choices can substantially change predicted stress and deformation fields, reinforcing the need for systematic parameter control in comparative studies [2]. Across the broader literature, FEA has been used both for localized defect repair and for global strengthening; however, many studies focus on either a single material system or a limited set of angles, which makes cross-material comparisons difficult. In parallel, analytical approaches for repair evaluation have continued to evolve: Soykök provided a recent analytical treatment of composite hand-layup repairs using energy-release-rate relations to evaluate repaired regions, underscoring that failure behavior may be governed by damage growth and interface effects rather than by simple stress limits alone [8]. These contributions collectively highlight that accurate prediction requires an integrated workflow that

is explicit about boundary conditions, interface assumptions, and how “failure” is defined in hybrid steel–composite systems.

2.4. Research Gap and Contribution of the Present Study

Despite extensive prior work on composite repairs and filament-wound composite pipes, two gaps remain important for practical pipeline rehabilitation. First, there is limited systematic comparison of multiple commercially relevant composite systems (e.g., glass-based wet layups versus UD prepregs versus woven fabrics) within a single modeling framework under consistent boundary conditions and a consistent burst criterion. Second, many studies emphasize laminate failure criteria within the composite, whereas pipeline integrity in repair scenarios is often governed by the steel substrate and the extent to which the overwrap reduces the steel’s demand under pressure. The present study addresses these gaps by establishing a validated coupled ANSYS Mechanical–ACP workflow and executing a controlled parametric sweep of outer-ply winding angle across four material systems, enabling a direct “angle–performance” comparison using the same steel-driven burst definition adopted throughout the simulations.

2.5. Research Objectives

The primary goals of this study are to:

- **Establish a computational framework** within ANSYS to simulate the reinforcement of petroleum-grade steel pipes using diverse composite materials (specifically Glass and Carbon fiber systems).
- **Quantify the impact of fiber orientation**, specifically analyzing how the wrapping angle of the outer ply dictates the pipe’s capacity to resist internal hydrostatic pressure.
- **Isolate the optimal design configuration** by comparing material performance and ply angles to define the exact setup that maximizes burst pressure (defined as the point where the steel core exceeds its Ultimate Tensile Strength).

3. METHODOLOGY

This study employs a validated finite element analysis (FEA) framework to quantify the influence of fiber orientation on the burst capacity of composite-

wrapped steel pipelines. All simulations were conducted in ANSYS Workbench 2025 R2, using a coupled workflow between ANSYS ACP (Pre) for composite layup definition and ANSYS Mechanical – Static Structural for global stress analysis. The methodology comprises: (i) definition of the steel pipe geometries, (ii) specification of isotropic and orthotropic material models, (iii) finite-element discretization and interface modelling, (iv) boundary conditions and loading, (v) failure criteria and post-processing, (vi) model validation against Barlow’s equation using a thin-walled reference pipe, and (vii) a parametric study on fiber orientation and material choice.

3.1. Geometrical Models

Two geometrical configurations were analysed: a validation pipe for benchmarking the numerical model against Barlow’s equation, and a production pipe for the composite reinforcement study.

3.1.1. Validation Pipe (Thin-Walled Baseline)

For model validation, a thin-walled steel pipe was generated in ANSYS SpaceClaim with the following dimensions: Length $L=2000$ mm, Outer diameter $D=100$ mm, Wall thickness $t=3$ mm, The thickness-to-diameter ratio $t/D=0.03<0.05$. $t/D<0.05$ satisfies the thin-walled assumption required for the application of Barlow’s equation. This configuration was used exclusively to verify the static structural modelling approach by comparing the numerically predicted burst pressure against the analytical solution.

3.1.2. Production Pipe (Composite-Wrapped Pipeline)

The main parametric study was performed on a production-grade pipeline geometry representative of petroleum transport lines: Length $L=1.5$ m, Outer diameter $D=168.3$ mm, Wall thickness $t=7.1$ mm

Table 1: Mechanical Properties of Structural Steel (pipe core) used in the Simulations.

Property	Symbol	Value
Young’s modulus	E	200 GPa
Poisson’s ratio	ν	0.30
Density	ρ	7850 kg/m ³
Tensile yield strength	σ_y	250 MPa
Ultimate tensile strength	σ_u	460 MPa

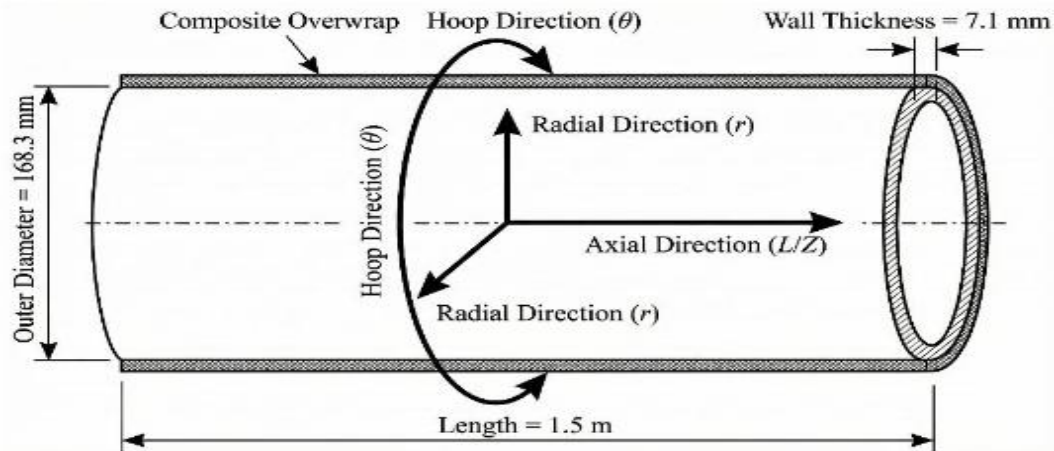


Figure 1: Pipe Geometry and Coordinate System.

Table 2: Key Orthotropic Properties of Composite Overwrap Materials (from ANSYS Engineering Data).

Material system	E_x (GPa)	E_y (GPa)	G_{xy} (GPa)	ν_{xy}	ρ (kg/m ³)	V_f	Form / note
Epoxy / E-Glass UD (wet)	35	9	3.5	0.28	2000	0.55	Baseline glass system
Epoxy / S-Glass UD	55	16	7.6	0.28	1990	0.55	Higher stiffness than E-Glass
Epoxy / Carbon UD (T300, 230 GPa)	121	8.6	4.7	0.27	1490	0.60	High-modulus UD tape
Epoxy / Carbon Woven (T300, 230 GPa)	61	61	6.5	0.04	1420	0.55	Bidirectional woven fabric

The composite overwrap was applied as a thin cylindrical shell bonded to the external surface of the steel pipe, covering the full length of the modelled section. A global cylindrical coordinate system was defined with the axial direction along the pipe axis, the hoop direction along the circumferential direction, and the radial direction-oriented outward from the pipe centreline (illustrated schematically in Figure 1).

3.2. Material Models

The hybrid system consists of an isotropic steel core and four orthotropic composite overwrap systems. All material data were taken from the ANSYS Engineering Data library to reflect commercially available repair materials.

3.2.1. Structural Steel (Pipe Core)

The steel pipe was modelled as an isotropic elastic-plastic material using the standard Structural Steel definition from ANSYS. The elastic-plastic behaviour is characterised by a linear elastic region followed by plastic yielding governed by a von Mises criterion. The key properties used in the simulations are summarised in Table 1.

These values are consistent with the material definition used in the validation study (Section 3.6), where the ultimate tensile strength $\sigma_u=460$ MPa was used as the reference for defining the burst condition.

3.2.2. Composite Overwrap Systems

Four composite systems were selected to span the practical spectrum of pipeline repair materials: Epoxy E-Glass Wet, Epoxy S-Glass UD, Epoxy Carbon UD (230 GPa) prepreg, and Epoxy Carbon Woven (230 GPa) prepreg. Each was modelled as a linear orthotropic elastic material in ANSYS, with the primary material axis aligned with the fiber direction.

Key stiffness parameters longitudinal modulus E_x , transverse moduli E_y , E_z , and shear moduli G_{xy} , G_{yz} , and G_{zx} were taken directly from the corresponding ANSYS Engineering Data entries. For clarity, Table 2 summarises the longitudinal modulus and density, which are most influential for the present burst-pressure analysis.

Full orthotropic elastic constants and strength parameters (tension/compression in fiber and transverse directions) are available from the ANSYS material definitions and can be reported in extended

tables if required by the journal. The present study focuses on comparative trends under elastic response and steel-driven yielding, rather than composite failure modes.

3.3. Finite Element Discretization

The steel pipe and composite overwrap were discretized in ANSYS Mechanical using three-dimensional solid and shell-type elements to capture both through-thickness and in-plane behaviour. For the production geometry:

The steel pipe was represented using 3D quadratic solid elements (e.g., SOLID186-type) with at least two elements through the wall thickness to resolve stress gradients. The composite overwrap was represented as a layered shell/solid region imported from ACP (Pre), with each ply defined by its orientation, thickness (1 mm), and material assignment.

A global element edge length of approximately 0.01 m was adopted for the pipe and overwrap, providing a balance between solution accuracy and computational cost while ensuring compatible mesh density at the steel–composite interface. The same meshing strategy was applied to both validation and production geometries to maintain consistency across simulations. Figure 2 illustrates the finite element mesh and the principal directions in the steel–composite assembly. The selected mesh density was kept consistent across all simulations to ensure fair comparison among material–angle combinations. Moreover, the model was first benchmarked against Barlow’s equation with acceptable agreement, providing confidence that the

adopted discretization is adequate for capturing the global burst-pressure trends studied here.

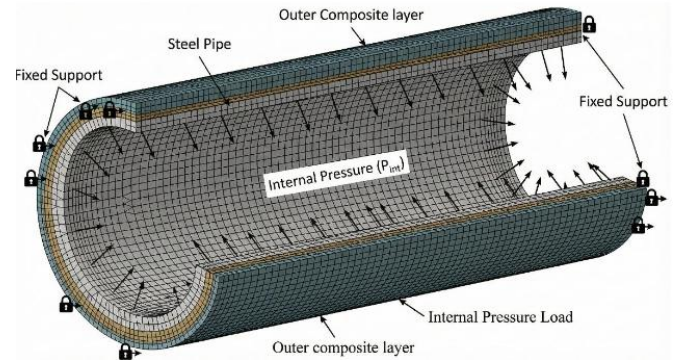


Figure 2: FEA model: Mesh + Boundary Conditions + Internal Pressure.

3.4 Composite Layup Definition in ANSYS ACP (Pre)

The composite laminate was defined in ANSYS ACP (Pre) following a hierarchical workflow and then mapped onto the 3D pipe surface, with each composite system from Table 2 assigned to a fabric definition using a nominal ply thickness of 1 mm; a cylindrical rosette (Rosette.1) was defined such that the 0° direction coincides with the pipe axis and 90° follows the hoop direction to ensure consistent interpretation of ply angles across all simulations; the outer surface of the pipe was defined as an oriented selection set (e.g., “composite outer”) to which the fabric and rosette definitions were mapped; and the laminate was constructed as a two-ply layup within the Modelling Group, comprising Ply 1 (inner) at 0° (aligned with the pipe axis) and held constant for all configurations, and Ply 2 (outer) with a

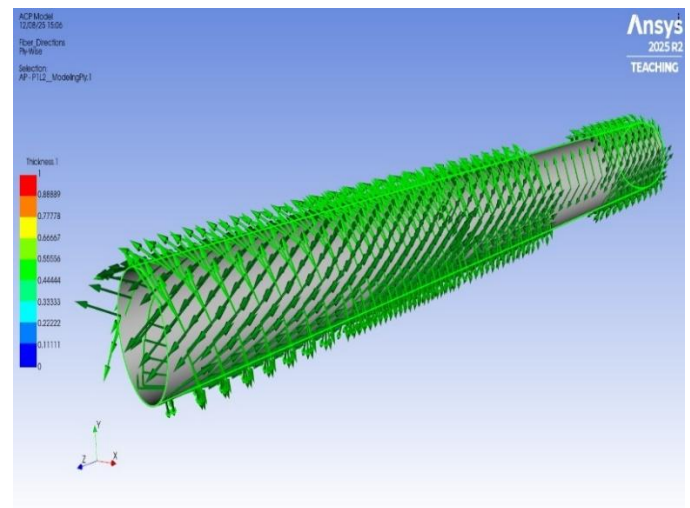
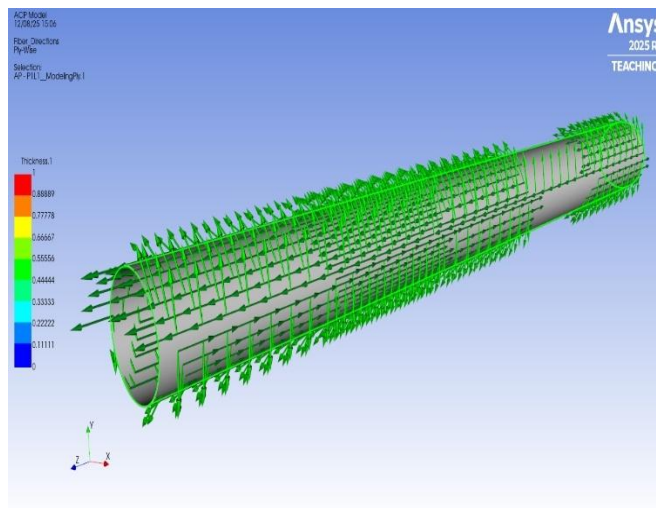


Figure 3: Composite Fabric Layers at 0 Degree and 25 Degrees in Ansys ACP (Pre).

variable orientation $\theta \in \{25^\circ, 35^\circ, 45^\circ, 55^\circ, 65^\circ, 75^\circ, 90^\circ\}$ used as the primary design parameter, with the resulting layup and principal directions shown schematically in Figure 3 this setup cleanly separates the baseline 0° inner layer from the parametric outer layer, allowing the influence of the second ply's angle to be systematically isolated.

The present study intentionally adopted a simplified two-ply laminate architecture to isolate the influence of the outer-ply winding angle and material topology on burst performance. By fixing the inner ply at 0° and varying only the outer-ply orientation, the framework allows a direct comparison of angle-dependent reinforcement behavior without introducing additional complexity associated with multilayer stacking interactions. Although multilayer laminates may further enhance confinement, stiffness tailoring, and stress redistribution, they also introduce additional variables such as inter-ply interaction, sequence dependency, and thickness effects. Therefore, the two-ply configuration serves as a controlled baseline for identifying the fundamental angle–performance trends prior to extending the framework toward more complex multilayer repair architectures.

3.5. Boundary Conditions and Loading

The structural model was transferred from ACP (Pre) into ANSYS Mechanical via the “Imported Plies” interface, preserving ply thickness, orientations, and material assignments, and the following boundary conditions and loadings were applied to both the validation and production models: the two end faces of the steel pipe were constrained with fixed supports to represent a pipeline segment axially restrained by adjacent sections (this intentionally introduces end effects, which were mitigated in post-processing by using averaged quantities over a mid-span gauge region as described in Section 3.6); a uniform internal pressure load was applied to all internal steel surfaces, with the pressure magnitude parameterized and incrementally increased until the burst condition was met; and the steel–composite interface between the steel outer surface and the composite overwrap was modelled as a perfectly bonded contact (no relative slip or separation), reflecting an assumed ideal adhesive bond and providing an upper bound on repair performance, with Figure 2 annotating the fixed end constraints and the internal pressure application regions.

The steels–composite interface was idealized as perfectly bonded in order to isolate the influence of fiber

orientation and material topology on burst performance. This assumption provides an upper-bound estimate of reinforcement efficiency because it neglects possible interfacial slip, debonding, and adhesive degradation that may develop under long-term service, thermal aging, moisture exposure, or repeated pressure cycling. In real pipeline repair systems, such interface deterioration can reduce stress transfer from the steel substrate to the composite overwrap, increase local shear concentration, and lower the effective burst pressure. Therefore, while the present model is appropriate for comparative angle–performance screening, the predicted burst capacities should be interpreted as idealized values representing a well-adhered repair condition.

3.6 Failure Criterion and Post-Processing

Since the primary structural risk in reinforced pipelines is yielding and rupture of the steel core, the failure assessment focused on the ductile steel rather than composite failure, and the following criterion was adopted: the equivalent von Mises stress in the steel domain was used as the primary indicator of yielding; to minimize artefacts from stress concentrations at the fixed ends, a central gauge region comprising the middle 50% of the pipe length was defined; and for each pressure level, a volume-weighted average of von Mises stress in the steel elements within this gauge region was computed.

The burst pressure p_{burst} was then defined as:

$$p_{\text{burst}} = \min\{p: \sigma^{\text{VM}}(p) \geq \sigma_u\}$$

where $\sigma^{\text{VM}}(p)$ is the average von Mises stress at pressure and $\sigma_u = 460$ MPa is the steel ultimate tensile strength (Table 1). This approach avoids interpretation based on local, end-induced peak stresses and yields a physically meaningful measure of global yielding relevant to burst capacity.

The present study defines failure primarily through yielding of the steel substrate because the principal objective is to evaluate the global burst resistance of the reinforced pipeline system. However, in practical composite repair applications, additional composite-related failure modes may also occur, including matrix cracking, fiber rupture, interfacial debonding, and interlaminar delamination. These mechanisms can influence local stress redistribution and progressive damage evolution, particularly under cyclic loading or environmental degradation. While such failure modes

were not explicitly modeled in the current framework, the adopted steel-driven criterion remains appropriate for comparative evaluation of the relative angle–performance behavior investigated in this study. Future work should incorporate progressive composite damage models and advanced failure criteria such as Hashin or Tsai–Wu formulations to capture coupled steel–composite failure mechanisms more comprehensively.

3.7. Model Validation Against Barlow's Equation

Prior to the composite parametric study, the finite element framework was validated against the classical thin-walled cylinder formulation. For the validation pipe described in Section 3.1.1, the analytical burst pressure was computed from Barlow's equation:

$$P = \frac{2\sigma_u t}{D}$$

where $t=3$ mm, $D=100$ mm and $\sigma_u=460$ MPa. This yields a theoretical bursting pressure of 13.8 MPa.

The same geometry and material definition were analysed using the static structural model described in Sections 3.3–3.6. By incrementally increasing the internal pressure and evaluating the average von Mises stress in the mid-span gauge region, the numerical burst pressure was determined to be 15.75 MPa, corresponding to the point at which the average von Mises stress exceeded σ_u as shown in Figure 4. The discrepancy between the analytical and numerical results ($\approx 14.13\%$) is attributed primarily to the idealized fixed-end boundary conditions and the three-dimensional stress state, and was considered acceptable for the purposes of this study.

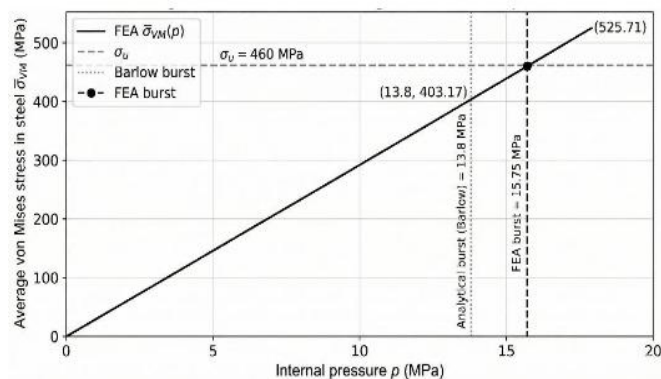


Figure 4: Model Validation Against Barlow's Equation.

The observed discrepancy between the analytical prediction and the finite element result is primarily associated with the simplifying assumptions embedded

in Barlow's equation. The analytical formulation assumes a perfectly thin-walled cylinder subjected to uniform membrane stresses and neglects three-dimensional constraint effects, localized stress redistribution, and end-boundary influences. In contrast, the present finite element model incorporates fixed-end constraints, through-thickness stress variation, and multiaxial stress states that more closely represent the physical behavior of restrained pipeline sections. Consequently, the numerical model predicts a slightly higher burst pressure than the idealized analytical solution. From an engineering perspective, the approximately 14.13% deviation is considered acceptable for validating the global structural response of the simulation framework. Similar discrepancies between analytical thin-wall solutions and three-dimensional finite element models are commonly reported in pipeline and pressure-vessel studies due to differences in boundary conditions and stress-state assumptions. Importantly, the purpose of the validation exercise was not to reproduce the exact analytical value, but rather to confirm that the numerical framework captures the correct burst-pressure trend and produces physically consistent results within an acceptable engineering tolerance.

Furthermore, the validated framework was used consistently across all parametric cases, meaning that the comparative angle–performance relationships presented in this study are governed by relative trends rather than absolute pressure magnitudes alone. Since all material systems and winding-angle configurations were evaluated using the same geometry, meshing strategy, boundary conditions, and failure criterion, the framework remains reliable for identifying the optimum reinforcement configurations and comparing the relative effectiveness of different composite architectures.

Although the present study is primarily numerical, the predicted trends are consistent with published experimental observations on composite pipe repair and filament-wound pressure vessels. Previous experimental and numerical studies have shown that laminate orientation, interface quality, and fiber topology strongly influence burst response under internal pressure, and that the optimum winding angle is application-dependent rather than universal. In particular, the present results agree with literature reports that unidirectional laminates often benefit from lower helical angles under constrained steel-substrate conditions, while woven architectures can respond more favorably to hoop-dominant loading because of their bidirectional load-sharing capability. Therefore, even in

the absence of new burst-test data in this work, the numerical outcomes are supported by existing experimental trends and remain suitable for comparative optimization of material–angle combinations.

3.8. Parametric Study: Fiber Orientation and Material Choice

Following validation, the framework was extended to the production pipe geometry for a systematic parametric study. For each of the four composite systems in Table 2: The inner ply was held fixed at 0° (axial), The outer ply angle θ was varied across {25°, 35°, 45°, 55°, 65°, 75°, 90°}, and the internal pressure was ramped until the burst criterion defined in Section 3.6 was met. For each (material, θ) combination, the resulting burst pressure was recorded, yielding a comprehensive angle–performance map used in the Results and Discussion sections to identify optimal fiber orientations and to compare the performance of glass- and carbon-based repair systems.

A high-level schematic of the simulation workflow—from geometry definition through ACP layout, Mechanical setup, solution, and post-processing is presented in Figure 5.

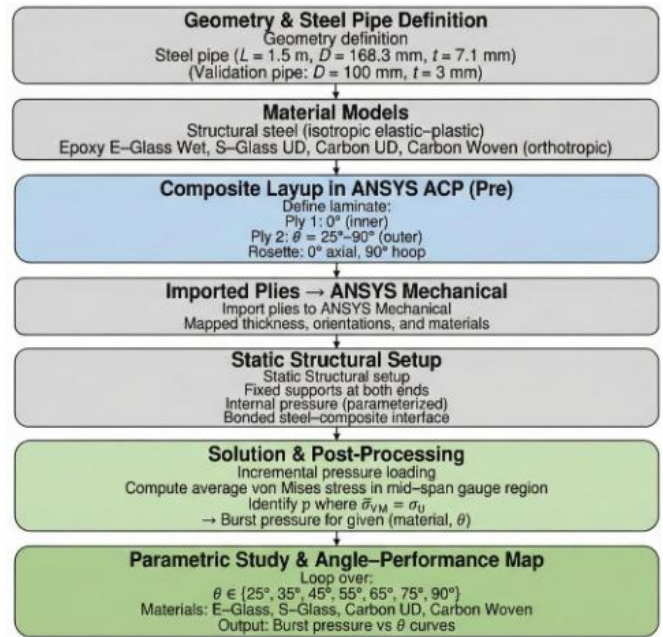


Figure 5: Simulation Workflow / Parametric Architecture.

4. RESULTS

This section reports the burst pressure (failure pressure) obtained from the parametric sweep of the outer-ply winding angle, $\theta \in \{25^\circ, 35^\circ, 45^\circ, 55^\circ, 65^\circ, 75^\circ, 90^\circ\}$, for four composite overwrap systems. For each

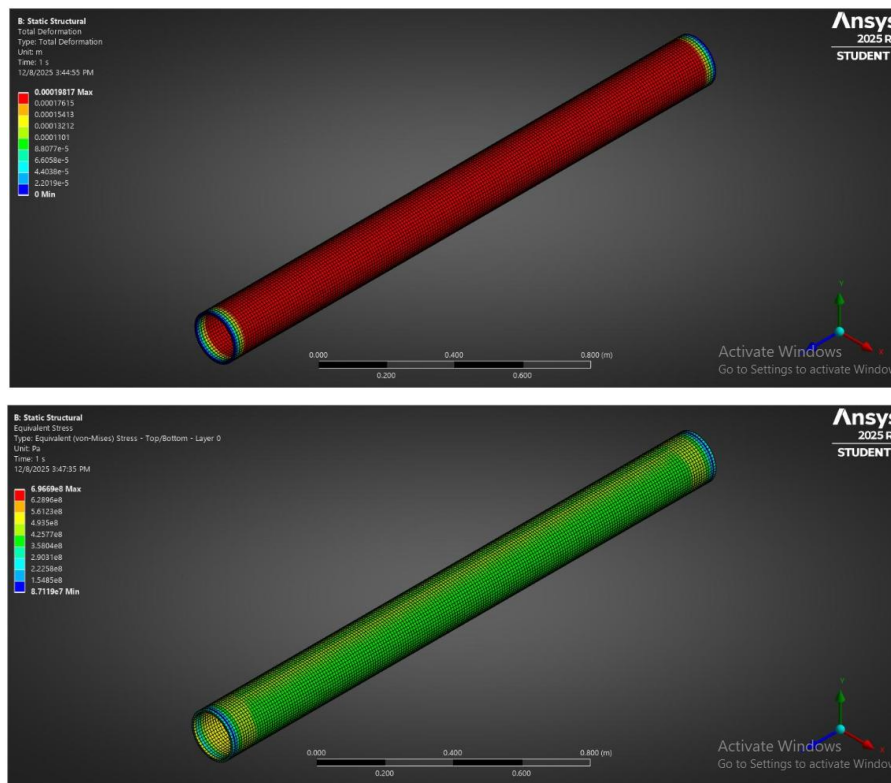


Figure 6: The Total Deformation and Equivalent Stress from an Individual Simulation is Visualized.

simulation, the internal pressure was incrementally increased until the burst criterion was satisfied (i.e., the average von Mises stress in the steel gauge region reached the steel ultimate tensile strength; see Section 3.6). Figure 6 presents a representative example of the deformation and equivalent stress fields at a near-failure pressure state, illustrating the global response of the steel–composite assembly.

4.1. Simulation A: Epoxy E-Glass Wet

This section reports the burst pressure (failure pressure) obtained from the parametric sweep of the all outer-ply winding angle, for four composite overwrap systems. For each simulation, the internal pressure was incrementally increased until the burst criterion was satisfied, defined as the average von Mises stress in the steel gauge region reaching the steel ultimate tensile strength (Section 3.6). Figure 7 presents a representative near-failure state, showing the total deformation and equivalent stress contours that characterize the global response of the steel–composite assembly.

For the Epoxy E-Glass Wet overwrap, the results show a consistent negative correlation between wrapping angle and bursting pressure. As the outer-ply orientation increased from a low-angle helical configuration (25°) toward a hoop-dominant wrap (90°), the burst pressure gradually decreased. The maximum burst pressure was recorded at 25°, reaching 47.8 MPa, while the minimum occurred at 90°, dropping to 47.17 MPa—corresponding to an overall reduction of approximately 1.3% relative to the 25° configuration.

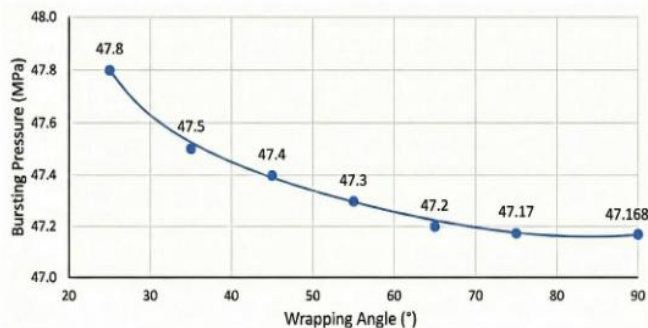


Figure 7: Variation of Bursting Pressure with Wrapping Angle for Epoxy E-Glass Wet.

4.2. Simulation B: Epoxy Carbon UD (230 GPa) Prepreg

The Epoxy E-Glass Wet overwrap showed a steady negative correlation between wrapping angle and burst

pressure: as the outer-ply orientation increased from a low-angle helical wrap (25°) toward a hoop-dominant wrap (90°), the pipe’s pressure capacity gradually decreased as shown in Figure 8. The maximum burst pressure occurred at 25°, reaching 47.8 MPa, while the minimum was recorded at 90° (47.17 MPa), corresponding to an overall reduction of approximately 1.3% relative to the 25° configuration.

In contrast to the E-Glass trend in terms of material class but with a similar angle-dependence, the Epoxy Carbon UD (230 GPa) prepreg system also exhibited a clear negative correlation between wrapping angle and burst pressure, with capacity decreasing as the outer ply shifted from a low helical angle (25°) toward a hoop orientation (90°). The highest burst pressure was achieved at 25° (51.24 MPa), whereas the lowest performance occurred at 90° (49.35 MPa). Although Carbon UD delivered the highest burst pressures among all evaluated materials, its reinforcing effectiveness in this two-ply configuration diminished as the fibers became increasingly perpendicular to the pipe axis, indicating that low-angle helical placement provides the most beneficial load-sharing with the longitudinal inner ply.

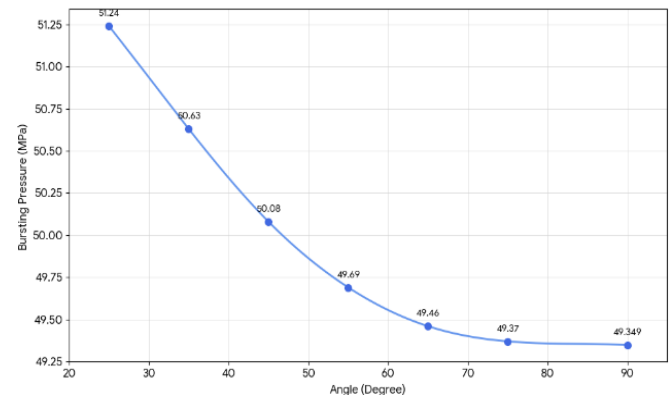


Figure 8: Variation of bursting Pressure with Wrapping Angle for Epoxy Carbon UD (230 GPa) Prepreg.

4.3. Simulation C: Epoxy Carbon Woven (230 GPa) Prepreg

For Epoxy Carbon Woven (230 GPa) Prepreg, the burst-pressure response shows a clear “U-shaped” trend with respect to the outer-ply winding angle as shown in Figure 9. The predicted capacity decreases slightly as the angle increases from 25° to about 45°, where the minimum burst pressure is reached at approximately 48.5 MPa, and then gradually recovers as the orientation approaches the hoop direction. The maximum burst pressure is obtained at 90° (49.15 MPa),

indicating that for woven fabrics the most effective configuration is hoop-dominant wrapping, where the bidirectional architecture aligns efficiently with the principal circumferential stress state.

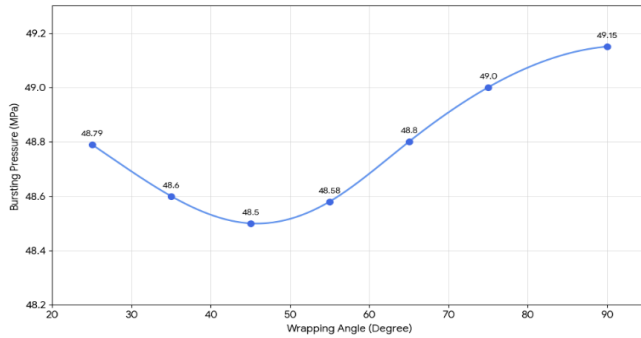


Figure 9: Variation of Bursting Pressure with Wrapping Angle for Epoxy Carbon Woven (230 GPa) Prepreg.

4.4. Simulation D: Epoxy S-Glass UD

The Epoxy S-Glass UD overwrap exhibited a trend closely matching the unidirectional carbon system, with the highest burst capacity occurring at low helical angles and a gradual decline as the outer-ply orientation approached a hoop wrap as shown in Figure 10. The maximum bursting pressure was 48.25 MPa at 25°, while the minimum value was 47.53 MPa at 90°, indicating a modest but consistent reduction in pressure capacity with increasing angle. Overall, S-Glass UD delivered reliable “mid-range” performance—typically stronger than the E-Glass wet system across the sweep, yet remaining below the peak performance achieved by Carbon UD in the same two-ply configuration

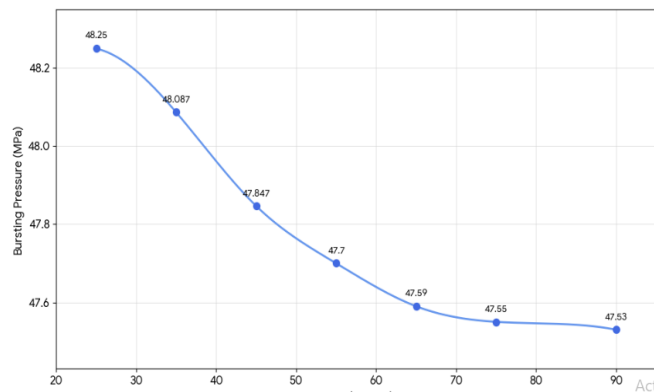


Figure 10: Variation of bursting Pressure with wrapping angle for Epoxy S-Glass UD.

5. DISCUSSIONS

The results in Section 4 reveal a clear dependence of burst pressure on both composite architecture

(unidirectional vs. woven) and outer-ply winding angle θ . Across the unidirectional systems (E-Glass Wet, S-Glass UD, and Carbon UD), the maximum burst capacity consistently occurred at the lowest tested helix angle (25°), followed by a gradual decline as the wrapping approached a hoop-dominant orientation (90) as shown in Table 3 and Figure 11. In contrast, the Carbon Woven system exhibited a non-monotonic response, with performance recovering toward 90° and reaching its peak in the hoop configuration. These trends indicate that the “optimal” orientation is not universal, but instead depends strongly on the interaction between the fixed 0° inner ply, the directional stiffness of the overwrap, and the steel-driven burst criterion based on the average von Mises stress in the gauge region.

Table 3: Comparative Bursting Pressure (MPa) vs. Wrapping Angle θ

Wrapping Angle (°)	Epoxy E-Glass Wet (MPa)	Epoxy Carbon UD (MPa)	Epoxy Carbon Woven (MPa)	Epoxy S-Glass UD (MPa)
25	47.8	51.24	48.8	48.25
35	47.5	50.63	48.6	48.087
45	47.4	50.08	48.5	47.847
55	47.3	49.69	48.58	47.7
65	47.2	49.46	48.78	47.59
75	47.17	49.37	49.0	47.55
90	47.168	49.35	49.15	47.53

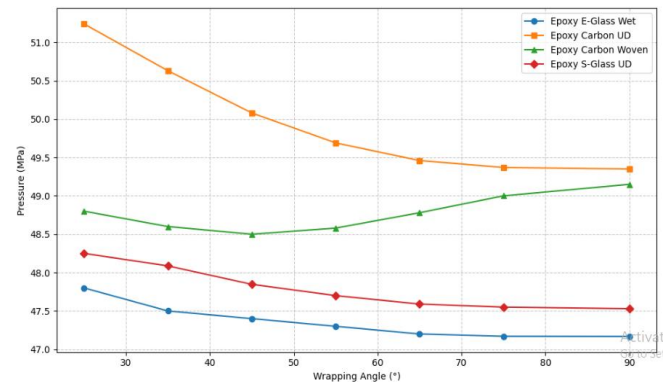


Figure 11: Variation of Bursting Pressure with Wrapping Angle for all Four Materials.

5.1. The "Helical Advantage": Why Unidirectional Composites Peak at 25°

One of the most distinct trends observed in this study was the dominance of the 25° helical wrapping angle across all unidirectional (UD) systems—Epoxy Carbon

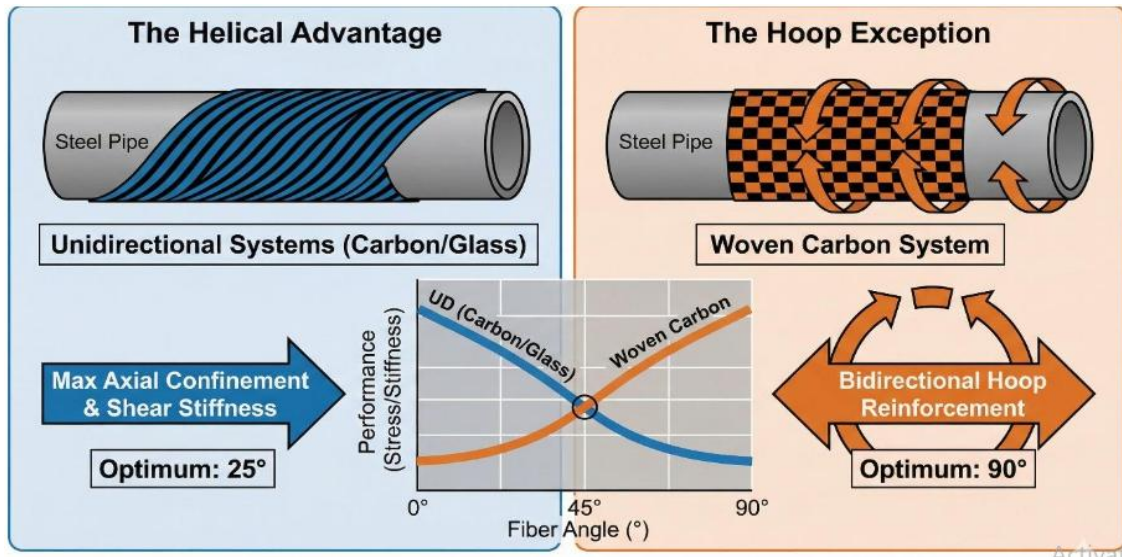


Figure 12: The Topology-Dependent Optimization Map.

UD, S-Glass UD, and E-Glass Wet. This finding is significant because it directly contradicts the "rule of thumb" often cited in classical netting analysis, which typically points to winding angles near $\pm 55^\circ$ as the ideal for pressure vessels.

However, the data suggests that for this specific two-layer architecture (where the inner ply is locked at 0°), the classical rule does not apply. Instead, the 25° outer ply essentially functions as a shear-stiffening truss. By wrapping at this lower angle, the outer layer physically constrains the steel pipe's tendency to bulge while simultaneously sharing the axial load. This creates a more efficient stress redistribution mechanism than a high-angle hoop wrap could achieve. While a 90° hoop wrap aligns perfectly with circumferential stress, it fails to offer the necessary longitudinal support. The 25° configuration strikes a better balance, effectively reducing the average Von Mises stress in the steel core and delaying the point at which the metal begins to yield.

The critical divergence in material performance is visually summarized in the optimization map in Figure 12. As illustrated, unidirectional materials (left panel) exhibit a 'Helical Advantage,' peaking at 25° where the inclined fibers act as a shear-stiffening truss to constrain the steel core. In contrast, the woven fabric (right panel) follows a 'Hoop Dominant' trend, achieving optimal performance at 90° due to its orthogonal weave pattern. This visual comparison underscores that the 'optimal angle' is not a fixed universal constant but a variable dependent on the fiber topology—specifically, whether the reinforcement acts as a unidirectional strap or a bidirectional mesh.

To further explain why unidirectional composites perform better at lower winding angles, the stress and strain distributions indicate that the 25° configuration provides more effective load sharing between the axial and hoop directions. Because the outer ply is inclined, it contributes not only circumferential confinement but also axial restraint, which reduces the localized stress level in the steel core and delays yielding. In contrast, the 90° configuration primarily resists hoop expansion, leaving the steel substrate more vulnerable to axial deformation and stress concentration, especially near the constrained end regions. The strain contours show the same tendency. At 25° , the deformation is distributed more uniformly through the steel-composite assembly, whereas at 90° the response becomes more localized, leading to earlier accumulation of equivalent stress in the steel. This explains why the unidirectional laminates reach their maximum burst pressure at low winding angles in the present two-ply architecture, where the inner 0° layer already provides baseline axial reinforcement.

5.2. The Woven Exception: Why Fabric Architecture Favors 90°

While the unidirectional tapes favored low angles, the Epoxy Carbon Woven material behaved completely differently, achieving its maximum burst pressure at a pure 90° hoop wrap. This divergence is not random; it is a direct result of the material's internal geometry.

Unlike UD tapes, which only have strength in one direction, the woven fabric is bidirectional. When we wrap a woven tape at 90° around a pipe, the "warp"

fibers align with the hoop direction (handling the pressure), but the "weft" fibers naturally align with the pipe's axis. In effect, a single layer of 90° woven fabric behaves like a pre-assembled 0°/90° laminate. This creates a natural load-sharing grid that stiffens the pipe in both principal directions simultaneously. Unidirectional laminates cannot do this; if we wrap them at 90°, we lose all axial contribution. The woven material's ability to "cheat" this trade-off allows it to maximize hoop confinement without sacrificing axial stability, making 90° the optimal orientation for fabrics.

The key distinction between woven and unidirectional laminates lies in how the fiber architecture redistributes load through the composite layer. In unidirectional tapes, the majority of stiffness and load-carrying capability exists only along the primary fiber direction, meaning that a hoop-oriented UD wrap sacrifices most axial reinforcement capability. In contrast, woven carbon contains orthogonal warp and weft fiber bundles that simultaneously contribute to both hoop and axial stiffness. As a result, the woven architecture promotes a more distributed transfer of stress between circumferential and longitudinal directions, reducing directional dependency and improving structural balance under internal pressure loading. This bidirectional load-sharing mechanism explains why the woven system remains effective at high hoop-dominant angles, whereas the unidirectional laminates exhibit reduced performance when oriented near 90°.

5.3. The Role of Material Stiffness in Burst Capacity

Beyond the geometric angles, the raw stiffness of the material proved to be a decisive factor in the pipe's survival. The Epoxy Carbon UD, with its massive axial modulus (~230 GPa), consistently outperformed the glass-based alternatives. It wasn't just about strength; the high modulus meant the carbon fibers could physically restrict the steel from expanding, keeping the strain levels low even under high pressure.

S-Glass UD served as a solid middle ground, edging out the E-Glass Wet by a small but consistent margin (roughly 0.5–1.0 MPa across the sweep). This reflects its superior tensile properties compared to standard commodity fiberglass. E-Glass Wet, while the lowest performer, still showed that geometry matters—optimizing the angle improved its results significantly. Ultimately, these findings confirm that while winding angle is critical, the fundamental modulus and tensile

limits of the fiber drive the upper ceiling of the reinforcement's potential.

Although some material systems exhibited relatively modest absolute changes in burst pressure across the angle sweep, the relative variations remain meaningful from an engineering design perspective. For example, the Carbon UD system exhibited an approximate 3.7% difference between its optimum and minimum configurations, while the glass-based systems showed smaller but still measurable variations. In pipeline rehabilitation applications, even small increases in allowable burst pressure can significantly affect safety margins, Maximum Allowable Operating Pressure (MAOP), and remaining service life. Therefore, the observed differences should be interpreted not only in terms of absolute pressure change, but also in terms of operational reliability and structural optimization under constrained field conditions.

5.4. Bridging the Gap: Comparisons with Historical and Modern Literature

When we place these results in the context of broader scientific research, we see a mix of convergence and necessary correction. Historical filament-winding theories—pioneered by figures like Xia, Takayanagi, and Kemmochi [5], and backed by experimental work from Soden, Kitching, and Tse [6]—rely heavily on netting analysis. This framework almost always dictates a $\pm 55^\circ$ optimum.

However, our results align much more closely with modern Finite Element investigations, such as those by Chen *et al.* [1] and Esmaeel and Taheri [4]. These contemporary studies argue that the "optimum" angle isn't a fixed mathematical constant derived from stress ratios. Instead, it is highly sensitive to the specific laminate architecture and the way the steel and composite transfer load between each other. Our finding that a 25° helical wrap is superior for UD materials supports the observations of Turai *et al.* [2] and Sulaiman *et al.* [7], who noted that boundary conditions and fiber orientation play a complex role that simple formula miss. Furthermore, our observation regarding the woven carbon peaking at 90° validates the mechanical logic proposed by Soykök [8], who emphasized that bidirectional reinforcement changes the damage propagation dynamics. In this light, this study does not just validate existing models; it provides a specific, numerically proven "angle-performance map" that updates older theories for modern repair materials.

6. IMPLICATIONS OF THIS STUDY

This study has a direct practical impact on how composite pipeline repairs should be designed and specified. For years, winding angles have often been selected using classical netting analysis and generic guidance (typically around $\pm 55^\circ$), but our results show that this can be unreliable for modern high-modulus prepreg systems. In particular, unidirectional composites performed best with a 25° helical wrap in this steel–composite architecture, which means repair effectiveness is not just about adding hoop stiffness—it depends on how well the wrap shares axial and shear loads with the steel substrate. From a field and standards perspective, this supports a shift away from “one-size-fits-all” prescriptions and toward guidelines that explicitly consider steel–composite interaction, rather than treating the wrap as an independent pressure vessel.

Operationally, the clearest message is that material selection must control the wrapping strategy. Woven carbon peaked at a 90° hoop wrap, while UD materials perform poorly at that same angle, so engineers can't apply a single angle rule across different repair inventories. Practically, that means using woven fabrics when hoop confinement is the priority, and using low-angle helical wraps when UD tapes are selected for structural stiffening. For operators, applying these optimized configurations can raise burst capacity and extend service life without cutting out pipe sections reducing shutdown time and avoiding hot-work risks. Just as importantly, the validated FEA workflow can be used as a pre-deployment “digital test” to screen repair choices quickly and cheaply, reducing the need for expensive trial builds and helping teams select the best angle–material combination even when budgets are limited (including cases where lower-cost systems like E-Glass can still deliver strong gains if oriented correctly).

7. CONCLUSION

This study successfully established a robust finite element framework for optimizing pipeline repairs, starting with a rigorous validation against Barlow's equation to ensure the simulation's fidelity. Although the validated finite element framework exhibited a moderate deviation from the idealized analytical solution, it consistently reproduced physically meaningful burst-pressure trends across all material and orientation configurations. With this baseline confirmed, we analyzed four distinct composite systems—ranging from

economical E-Glass to high-modulus Carbon UD—across a wide sweep of winding angles. The results revealed a sharp distinction in material behavior that contradicts a “one-size-fits-all” approach. While all unidirectional tapes (E-Glass, S-Glass, and Carbon UD) consistently maximized burst capacity at a 25° helical angle due to superior shear stiffening and confinement, the woven carbon fabric behaved uniquely. Because of its bidirectional weave, the woven material achieved its peak performance at a pure 90° hoop wrap, demonstrating that the “optimal angle” is dictated entirely by the specific fiber topology.

These findings directly challenge the standard industry reliance on classical netting analysis, suggesting that modern prepreg repairs require material-specific strategies rather than generic rules of thumb. By mapping these angle–performance relationships, we determined that a 25° configuration using Epoxy Carbon UD offers the highest overall burst resistance (51.24 MPa), though even cost-effective E-Glass systems show significant structural gains when oriented correctly. Ultimately, this work moves beyond theoretical simulation to provide a practical, numerically validated guide for field engineers, ensuring that pipeline reinforcement strategies are not only safer and more reliable but also rigorously optimized for the specific materials on hand.

8. LIMITATIONS AND FUTURE RESEARCH DIRECTIONS

While the present study establishes a validated numerical framework for evaluating burst-pressure enhancement in composite-overwrapped steel pipelines, the results should be interpreted within the context of several modelling assumptions. The simulations considered only static internal pressure loading, whereas real petroleum pipelines are often subjected to cyclic pressure fluctuations, fatigue loading, thermal gradients, and environmental exposure during long-term service. In addition, the steel–composite interface was idealized as perfectly bonded to isolate the influence of fiber orientation and material topology on burst behavior. Although this assumption provides a useful upper-bound estimate of reinforcement efficiency, it neglects possible interfacial slip, adhesive degradation, moisture-induced weakening, and progressive debonding that may occur in practical repair systems. Similarly, failure was defined primarily through yielding of the steel substrate using average von Mises stress, while additional composite-related failure modes such as matrix cracking, fiber rupture, and delamination

were not explicitly modeled. The study also employed a simplified two-ply laminate architecture and pristine pipeline geometry without corrosion defects, wall thinning, or manufacturing imperfections.

Future research should therefore extend the present framework toward greater industrial realism by incorporating cyclic internal pressure loading, thermal expansion mismatch, fatigue effects, and environmental degradation mechanisms. Experimental burst testing would also be valuable for further validating the numerical predictions and calibrating progressive damage behavior. Additional studies should investigate multilayer and hybrid laminate architectures, imperfect bonding conditions, and defected pipelines containing corrosion pits or wall-thinning damage. Furthermore, integrating cohesive-zone interface models and progressive composite failure criteria such as Hashin or Tsai–Wu formulations would improve prediction of coupled steel–composite failure mechanisms. Finally, automated optimization and machine-learning-assisted parameter selection may provide an efficient pathway for identifying optimum material–angle combinations for field-scale pipeline rehabilitation.

DECLARATIONS

AVAILABILITY OF DATA AND MATERIALS

The datasets generated will be made available upon reasonable request.

COMPETING INTERESTS

There is no financial competing interest in this research.

FUNDING

No funding information available.

ETHICS, CONSENT TO PARTICIPATE, AND CONSENT TO PUBLISH DECLARATIONS:

Not applicable

AUTHOR'S CONTRIBUTION

Samudra Jit Saha: Methodology, Software, Models, Simulation validation, Project administration, Data visualization, Data analysis, Writing-Original draft. **Marufa Akter:** Simulations, Data curation, Data visualization, Documentation. **Nowreen Jahan:** Simulations, Data curation, Data visualization, Documentation. **Sayma Islam:** Simulations, Data curation, Data visualization, Documentation. **Abid Chowdhury:** Simulations, Data visualization, Documentation. **Md. Abdus Shabur:** Conceptualization, Methodology, Graph plotting, Visualization, Supervision, Writing, Review and Editing

ACKNOWLEDGEMENTS

The authors would like to thank the Department of Robotics and Mechatronics Engineering for providing high speed computational facility and their overall support.

REFERENCES

- [1] Chen, J., Wang, H., Salemi, M., & Balaguru, P. N. (2021). Finite element analysis of composite repair for damaged steel pipeline. *Coatings*, 11(3), 301.
- [2] Turai, Y. S., *et al.* (2022). Finite Element Analysis on Wrapping Structure of Piping System. *Research Progress in Mechanical and Manufacturing Engineering*, 2(2), 150-159.
- [3] Alexander, C., & Francini, R. (2006). State of the art assessment of composite systems used to repair transmission pipelines. *Proceedings of the 6th International Pipeline Conference*, Calgary, AB, Canada.
- [4] Esmaeel, R. A., & Taheri, F. (2009). Stress analysis of a pressurized pipe repaired with a composite sleeve. *Journal of Pressure Vessel Technology*, 131(6).
- [5] Xia, M., Takayanagi, H., & Kemmochi, K. (2001). Analysis of multi-layered filament-wound composite pipes under internal pressure. *Composite Structures*, 53(4), 483-491.
- [6] Soden, P. D., Kitching, R., & Tse, P. C. (1989). Experimental failure stresses for +/- 55 deg filament wound glass fibre reinforced plastic tubes under biaxial loads. *Composites*, 20(2), 125-135.
- [7] Sulaiman, S., Borazjani, S., & Tang, S. H. (2013). Finite element analysis of filament-wound composite pressure vessels under internal pressure. *IOP Conference Series: Materials Science and Engineering*, 50(1).
- [8] Soykök, İ. F. (2025). Analytical Evaluation of the Strength in the Repair of Damaged Areas in Steel Pipes with the Composite Hand-Laying Method Using Energy Release Rate Relations. *Journal of Dynamics, Energy and Utility*, 1(2), 51-59.